Development of 3D Printable Composite Inks for Millimeter Wave Applications

Bradley Duncan, Maxwell Plaut, Benjamin Barclay, John Russo, and Theodore Fedynyshyn
Chemical, Microsystem, and Nanoscale Technologies Group
MIT Lincoln Laboratory
Lexington, MA, USA
bradley.duncan@ll.mit.edu, maxwell.plaut@ll.mit.edu, benjamin.barclay@ll.mit.edu, jar@ll.mit.edu, fedynyshyn@ll.mit.edu

Sebastien G. M. Uzel, Robert Weeks, and Jennifer A. Lewis
John A. Paulson School of Engineering and Applied Sciences
Harvard University
Cambridge, MA, USA
suzel@g.harvard.edu, rweeks@g.harvard.edu, jalewis@seas.harvard.edu

***Abstract*— This paper presents the development of a series of conductive and dielectric inks for 3D printing. The dielectric inks were found to possess dielectric constants ranging from 2 - 26.5 with loss tangents on the order of 10^{-4} - 10^{-2} over the 26.5 to 40 GHz range (K_a band). The fabrication of gradient dielectrics via a custom active mixing nozzle is also described.**

Keywords—3D printing; composites; gradient dielectrics; conductive traces; millimeter wave

I. INTRODUCTION

3D printing of RF devices offers a powerful strategy to generate structures not achievable through typical fabrication methods [1]. Previously, we have developed a triblock copolymer system for generating low loss dielectric structures via direct-write 3D printing [2]. By incorporating ceramic nanoparticles into the polymer matrix, the dielectric constant of the printed material could be increased [3]. Our progress in expanding our materials palette of low loss dielectric inks as well as the integration of complex materials deposition approaches into our printing process is described below.

II. MATERIALS AND CHARACTERIZATION

A. Composite Dielectrics

Our recent work has focused on increasing the dielectric constants of our inks while maintaining their low-loss characteristics. Our hypothesis was that by varying the ceramic nanoparticle content of our generated composite inks, we should be able to tune the dielectric constant of our printed structures. Hydrophobic styrene-isoprene-styrene (SIS) triblock polymers served as our model low dielectric polymer with a measured dielectric constant of 2.2 and loss tangent of 1.6 x 10^{-3}. We selected TiO_2 and $SrTiO_3$ nanoparticles due to their high dielectric constants and low loss tangents. The surfaces of ceramic nanoparticles were functionalized to facilitate improved blending into the polymer matrix. Inks were formulated by combining the polymer and nanoparticles in volatile organic solvents and extruding the viscoelastic ink out of micron-sized nozzles. Structures with 0 % to 60 % volume fractions of ceramics were tested to determine their dielectric constants in the K_a band.

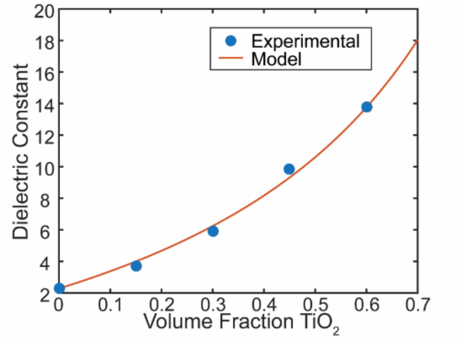

Fig. 1. Measured dielectric constant of TiO_2 composites

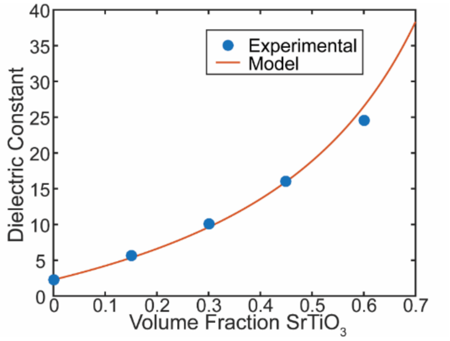

Fig. 2. Measured dielectric constants of $SrTiO_3$ composites

This material is based upon work supported by the Assistant Secretary of Defense for Research and Engineering under Air Force Contract No. FA8721-05-C-0002 and/or FA8702-15-D-0001. Any opinions, findings, conclusions or recommendations expressed in this material are those of the author(s) and do not necessarily reflect the views of the Assistant Secretary of Defense for Research and Engineering.

The S-parameters from 26.5 to 40 GHz of a WR-28 waveguide loaded with composite were measured to calculate the dielectric constants and loss tangents with Keysight's proprietary software. These materials demonstrated median dielectric constants from 2 – 26.5 and loss tangents on the order of 10^{-4} - 10^{-2} over the 26.5 to 40 GHz range as shown in Table I, Fig. 1, and Fig. 2. This behavior was dependent on the volume fraction of ceramic used and these results were modeled using effective medium theory [4] as:

$$\varepsilon = \varepsilon_B \left[1 + \frac{f_A(\varepsilon_A - \varepsilon_B)}{\varepsilon_B + n(1 - f_A)(\varepsilon_A - \varepsilon_B)}\right] \tag{1}$$

where ε is the effective permittivity of the composite, ε_A is the permittivity of the particle, ε_B is the permittivity of the polymer, f_a is the volumetric ratio of the particles within the polymer matrix, and n is the shape factor to account for particle morphology. From these data, we can predictively generate printable materials with a wide range of dielectric constants.

TABLE I. DIELECTRIC CHARACTERIZATION OF PRINTED COMPOSITES

Material (vol. %)	**Dielectric Constant (ε') (34 GHz)**	**Loss Tangent (ε"/ε') (34 GHz)**
SIS Polymer	2.2	0.002
TiO_2/SIS (15 : 85)	3.7	0.005
TiO_2/SIS (30 : 70)	5.9	0.012
TiO_2/SIS (45 : 55)	9.9	0.016
TiO_2/SIS (60 : 40)	13.8	0.028
$SrTiO_3$/SIS (15 : 85)	5.6	0.035
$SrTiO_3$/SIS (30 : 70)	10.1	0.032
$SrTiO_3$/SIS (45 : 55)	16.0	0.033
$SrTiO_3$/SIS (60 : 40)	24.6	0.050

B. *Conductive Composites*

Our polymer-based system has also demonstrated compatibility with metallic particles. By incorporating metal flakes into our inks we are able to print conductive structures. As shown in Fig. 3, self-supporting metal composite traces of 200 µm can be effectively generated. The conductivities of printed traces were determined using a 4-wire resistance measurement. As shown in Table II we are able to generate metal composite structures that possess conductivities that are ~9 % of bulk silver. Notably, these results were obtained without the need for high temperature sintering conditions so as to maintain compatibility with the polymer dielectrics.

TABLE II. SUMMARY OF ELECTRICAL DATA FOR PRINTED WIRES

Material	**Resistivity (Ω·m)**	**Conductivity (S/m)**	**% of Bulk Silver Conductivity**
Bulk Silver	$1.6 * 10^{-8}$	$6.3 * 10^{7}$	100
Commercial Silver Ink	$7.4 * 10^{-6}$	$1.4 * 10^{5}$	0.2
Silver Flake Ink	$1.8 * 10^{-7}$	$5.7 * 10^{6}$	9.1
Gold Flake Ink	$8.3 * 10^{-7}$	$1.2 * 10^{6}$	1.9

III. PRINTING METHODOLGY

To generate gradients of dielectrics, we have been developing a custom active mixing nozzle [5]. We are able to direct the dielectric constant of the final printed structure by varying the polymer-to-nanoparticle ratio within the ink on-the-fly. Two syringe pumps, one filled with a high dielectric ink and the other with a low dielectric ink are combined within a mixing chamber prior to extrusion. Both the syringe pumps and nozzle are controlled using an Aerotech system. As shown in Fig. 4, the extruded filament can be programmably controlled eliminating the sharp transitions from individual inks and allowing for both geometric and compositional control over printed structures.

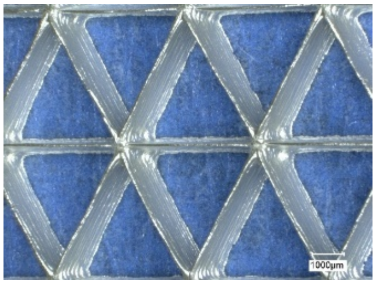

Fig. 3. Triangular lattice structure of printed silver composite

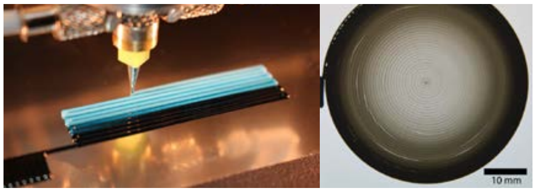

Fig. 4. Photograph of active mixing nozzle (left) and printed gradient

IV. CONCLUSIONS

We have developed a series of conductive and dielectric inks for 3D printing RF devices. Combinations of the conductive and high dielectric constant materials allows the fabrication of complex structures that traditional manufacturing strategies cannot achieve. Furthermore, the ability to control the dielectric constant of a structure in a truly gradient fashion in 3 dimensions opens up a variety of novel architectures not previously realized.

REFERENCES

[1] M. Liang and H. Xin, "Three-Dimensionally Printed/Additive Manufactured Antennas," in *Handbook of Antenna Technologies*, Z. N. Chen, D. Liu, H. Nakano, X. Qing, and T. Zwick, Eds., ed Singapore: Springer Singapore, 2016, pp. 661-697.

[2] M. Lis, M. Plaut, A. Zai, D. Cipolle, J. Russo, J. Lewis, *et al.*, "Polymer Dielectrics for 3D-Printed RF Devices in the Ka Band," *Adv. Mater. Technol.*, vol. 1, p. 1600027, 2016.

[3] M. Lis, M. Plaut, A. Zai, D. Cipolle, J. Russo, and T. Fedynyshyn, "High Performance, 3D-Printable Dielectric Nanocomposites for Millimeter Wave Devices," *ACS Appl. Mater. Interfaces*, vol. 8, pp. 34019-34026, Dec 2016.

[4] R. Yang, Q. Jianmin, T. Marinis, and C. P. Wong, "A precise numerical prediction of effective dielectric constant for polymer-ceramic composite based on effective-medium theory," *IEEE Transactions on Components and Packaging Technologies,* vol. 23, pp. 680-683, 2000.

[5] T. J. Ober, D. Foresti, and J. A. Lewis, "Active mixing of complex fluids at the microscale," *Proc Natl Acad Sci U S A,* vol. 112, pp. 12293-8, Oct 2015.